Neurosci. Bull. October, 2018, 34(5):736–746
https://doi.org/10.1007/s12264-018-0268-9

www.neurosci.cn
www.springer.com/12264

ORIGINAL ARTICLE

Sex Differences in Neuropathology and Cognitive Behavior in APP/PS1/tau Triple-Transgenic Mouse Model of Alzheimer's Disease

Jun-Ting Yang[1] · Zhao-Jun Wang[1] · Hong-Yan Cai[2] · Li Yuan[3] · Meng-Ming Hu[1] · Mei-Na Wu[1] · Jin-Shun Qi[1]

Received: 28 December 2017 / Accepted: 16 June 2018 / Published online: 11 August 2018

Abstract Alzheimer's disease (AD) is the most common form of dementia among the elderly, characterized by amyloid plaques, neurofibrillary tangles, and neuroinflammation in the brain, as well as impaired cognitive behaviors. A sex difference in the prevalence of AD has been noted, while sex differences in the cerebral pathology and relevant molecular mechanisms are not well clarified. In the present study, we systematically investigated the sex differences in pathological characteristics and cognitive behavior in 12-month-old male and female APP/PS1/tau triple-transgenic AD mice (3×Tg-AD mice) and examined the molecular mechanisms. We found that female 3×Tg-AD mice displayed more prominent amyloid plaques, neurofibrillary tangles, neuroinflammation, and spatial cognitive deficits than male 3×Tg-AD mice. Furthermore, the expression levels of hippocampal protein kinase A–cAMP response element-binding protein (PKA-CREB) and p38–mitogen-activated protein kinases (MAPK) also showed sex difference in the AD mice, with a significant increase in the levels of p-PKA/p-CREB and a decrease in the p-p38 in female, but not male, 3×Tg-AD mice. We suggest that an estrogen deficiency-induced PKA-CREB-MAPK signaling disorder in 12-month-old female 3×Tg-AD mice might be involved in the serious pathological and cognitive damage in these mice. Therefore, sex differences should be taken into account in investigating AD biomarkers and related target molecules, and estrogen supplementation or PKA-CREB-MAPK stabilization could be beneficial in relieving the pathological damage in AD and improving the cognitive behavior of reproductively-senescent females.

Keywords Sex difference · 3×Tg-AD mouse · Amyloid plaque · Neurofibrillary tangle · Neuroinflammation · Spatial memory

Introduction

Alzheimer's disease (AD) is a progressive and irreversible neurodegenerative disorder characterized by memory loss and cognitive decline [1]. Its pathological features include a high density of senile plaques, neurofibrillary tangles, and neuroinflammation in the brain. Amyloid β (Aβ) peptides, cleaved from amyloid precursor protein (APP) by β- and γ-secretases, are the main components of senile plaques and play a key role in the onset and progression of AD [2, 3]. Hyperphosphorylated tau protein, the main component of neurofibrillary tangles in neurons, ultimately leads to neuronal death [4]. Moreover, a highly significant correlation has been found between the number of neurofibrillary tangles and the severity of dementia [5]. The neurotoxic Aβ and hyperphosphorylated tau increase the levels of pro-inflammatory cytokines in the brain and lead to neuronal damage or death, which induces further activation of glial cells and results in a self-propagating, detrimental cycle of neuroinflammation and neurodegeneration [6]. Taken

Jun-Ting Yang and Zhao-Jun Wang have contributed equally to this work.

✉ Mei-Na Wu
wmna@163.com

✉ Jin-Shun Qi
jinshunqi2009@163.com

[1] Department of Physiology, Shanxi Medical University, Taiyuan 030001, China

[2] Department of Microbiology and Immunology, Shanxi Medical University, Taiyuan 030001, China

[3] Department of Physiology, Changzhi Medical College, Changzhi 046000, China

together, the Aβ accumulation and tau hyperphosphorylation, as well as neuroinflammation, constitute the major pathological characteristics of AD.

Sex differences in the prevalence, risk, and severity in AD patients have been demonstrated in numerous studies. Epidemiological and clinical studies have provided evidence for these differences, women being more susceptible to developing AD than men [7]. Both neuroimaging and postmortem human studies have revealed that the pathology of AD is stronger in women than in men [8]. Most currently, Koran *et al*. reported an interaction between sex and total tau levels in longitudinal hippocampal atrophy, and found that women with $A\beta_{1\text{-}42}$ and total tau levels indicative of worse pathological changes showed more rapid hippocampal atrophy [9]. Although sex differences have been reported in AD patients, there is still a lack of systematic pathological evidence from assessing Aβ plaques, phosphorylated tau, and neuroinflammation in the same AD animals. Besides, the sex differences in the tau protein levels in AD patients and animals are controversial. For instance, Koppel *et al*. precisely quantified tau abnormalities in postmortem samples from psychotic AD patients, and found that females, but not males, had significantly higher levels of phosphorylated tau in the frontal cortex [10]. Carroll *et al*. reported a most pronounced sex difference in Aβ accumulation in the frontal cortex of 6–8 month-old AD mice, with higher Aβ levels and more severe cognitive deficits in females than age-matched males [11], but they did not test the levels of phosphorylated tau because of the age of the mice they used. At almost the same time, Hirata-Fukae and colleagues reported that females exhibit more extensive amyloid, but not tau, pathology in a transgenic AD model [12]. In view of the facts that the hippocampus is the key central area most severely affected by increased AD biomarkers and that there is a high correlation between the severity of dementia and the number of neurofibrillary tangles [5], it is still necessary to further clarify the sex differences in the neuropathological characteristics of the hippocampus in the transgenic mouse model of AD. The present study systematically compared the pathological Aβ, phosphorylated tau, and neuroinflammation in the brain between male and female 3×Tg-AD mice. The sex differences in cognitive behavior and pathology-related molecular mechanisms were also investigated.

Materials and Methods

Animals

APP/PS1/tau 3×Tg-AD mice over-expressing mutant APP (APP_{SWE}), presenilin 1 ($PS1_{M146V}$), and tau (tau_{P301L}) were obtained from the Jackson Laboratory (Bar Harbor, ME). Age-matched C57 wild-type (WT) mice served as normal controls. All animals were bred in the Research Animal Center of Shanxi Medical University and the procedures were approved by the Shanxi Committee on Ethics in Animal Research. The animals were maintained under a 12/12-h light/dark cycle at 23 ± 1 °C and 60% relative humidity. Food and water were available *ad libitum*. The mice were divided into four groups according to transgene and sex: WT + Male, WT + Female, 3×Tg-AD + Male, and 3×Tg-AD + Female. In the pathological examinations, $n = 6$/group, and in the behavioral tests, $n = 10$/group.

Immunohistochemistry

The mice were sacrificed by cardiac perfusion-fixation with phosphate-buffered saline (PBS) and 4% paraformaldehyde (PFA). For frozen section experiments, the left hemisphere was fixed in 4% PFA (pH 7.4) for 24 h and incubated in 30% sucrose at room temperature for another 24 h. Immediately afterward, the tissues were embedded in OCT frozen embedding medium (Heidelberger Strasse 17-19, Nussloch, Germany). Coronal sections were cut at 25 μm on a freezing microtome (Leica, CM1850) and stored at 4 °C in PBS. Then, the sections were incubated with 5% hydrogen peroxide at room temperature for 15 min and blocked with 5% goat serum (Solarbio, Beijing, China) for 30 min. The sections were incubated with primary antibodies (anti-$A\beta_{1\text{-}16}$, 6E10, dilution 1:500, 803105, Biolegend; anti-GFAP, 1:200, bs-0199R, Bioss, Beijing, China; anti-Iba-1, 1:200, 019-19741, Wako Pure Chemical Industries, Ltd, Japan) overnight at 4 °C, followed by incubation with secondary antibody (peroxidase-conjugated Affinipure goat anti-rabbit IgG (H + L), 1:200, ZSGB-BIO, Beijing, China) at 37 °C for 2 h. For paraffin section experiments, the other hemisphere was processed into paraffin-embedded blocks. Sections were cut at 2 μm on a Leica microtome (RM2255) and attached to glass slides. The paraffin was removed with xylene. Next, the tissues were rehydrated in 100%, 90%, 80%, 70%, and 50% ethanol and washed twice with distilled water. Then, the sections were incubated with 3% hydrogen peroxide at room temperature for 15 min, and heated in a microwave oven for 3 min with pH 6.0 citrate acid buffer. The sections were washed three times (15 min each) with PBS (0.5% TritonX-100) and blocked with 5% goat serum for 30 min. The sections were incubated with monoclonal anti-tau (phospho-T231) antibody (1:200, ab151559, Abcam, Cambridge, UK) at 37 °C for 1 h, and then with secondary antibody (peroxidase-conjugated Affinipure goat anti-rabbit IgG (H + L), 1:200, ZSGB-BIO) at 37 °C for 20 min. The diaminobenzidine method was used for positive cell and positive area staining. The average percentage area of

antigen-antibody complexes and the average numbers of cells positive for anti-p-tau were measured using Image-Pro Plus 6.0 (Fryer, Huntley, IL) from at least three hippocampal sections per mouse.

Western Blotting

The hippocampi of mice were dissected and the proteins extracted (Tissue Protein Extraction Reagent; Boster, Beijing, China) and supplemented with complete protease inhibitor (Boster). The protein concentration was measured using a bicinchoninic acid protein assay kit after removing debris by low-speed centrifugation. A 30-μg protein sample was separated on 12% SDS–polyacrylamide gel. After electrophoresis, proteins were transferred onto a PVDF membrane and nonspecific binding was blocked with 5% BSA in Tris-buffered saline containing 0.05% Tween-20 (TBST). The membrane was incubated with the primary antibody overnight at 4 °C, followed by the secondary antibody at room temperature for 2 h. The following primary antibodies (all from Abcam) were used: monoclonal anti-phospho-PKA (1:1000), monoclonal anti-PKA (1:1000); monoclonal anti-phospho-CREB (1:2500), monoclonal anti-CREB (1:1000), monoclonal anti-phospho-p38 (1:1000), and monoclonal anti-p38 (1:1000). GAPDH and β-actin were used as loading controls. The secondary antibody was anti-rabbit IgG-HRP (1:5000, ZSGB-BIO). The membrane was rinsed with TBST and the immunocomplex was visualized using an enhanced chemiluminescence detection kit (Beyotime, Shanghai, China). The signals on the membrane were scanned with a FluorChem scanner (ProteinSimple) and quantified with Alpha View SA software (Azure C300 Biosystems, Inc, USA).

Morris Water Maze (MWM) Test

The MWM test was conducted to examine spatial learning and memory. The MWM comprised a circular pool (Zhenghua Bio Instruments Ltd., Huaibei, China), an automatic camera, and an analysis system [13]. The pool (1.2 m in diameter) was filled with non-toxic opaque water to a depth of 50 cm. The water temperature was adjusted to 23 ± 2 °C. The MWM was divided into four equal quadrants, and four different equidistant visual cues were placed on the inner wall of the pool for mouse positioning. The cylindrical escape platform (12 cm in diameter) was placed in the center of a designated quadrant with its top 1 cm below the water surface. After 7 days of environmental adaptation, the mice were first trained for 5 consecutive days on spatial learning. In the hidden-platform test, each mouse received 4 trials per day to find the submerged platform at a fixed quadrant center and escape latencies were recorded as the arithmetic mean of the 4 trials. In each training unit, the mouse was placed into the water facing the pool wall, and allowed to swim freely to the escape platform. After reaching the platform, the mouse was allowed to stay there for 5 s. If it failed to find the platform within 60 s, the mouse was manually guided and allowed to stay on the platform for 30 s. The mouse was subsequently returned to the home cage for 60 s before the next trial. A probe test for spatial memory was conducted on day 6. The platform was removed and the swimming time was limited to 60 s. The escape latency (s), the time in target quadrant, and swimming speed (cm/s) were recorded and analyzed with Ethovision 3.0 software (Noldus Information Technology, Wageningen, Netherlands).

Statistics

All values are expressed as mean ± standard error (SEM). For the MWM tests, the escape latencies were analyzed using three-way repeated measures analysis of variance (ANOVA). SPSS 13.0 (SPSS Inc., Chicago, IL) and SigmaPlot 11.0 (Jandel Scientifi, Costa Madre, CA) were used for statistical analyses. The data were analyzed by two-way repeated measures ANOVA and Tukey's *post hoc* test. The significance level was set at $P < 0.05$.

Results

Female 3×Tg-AD Mice Showed More Amyloid Plaques in the Hippocampus

Aβ plaques are the main pathological biomarker of AD. Representative immunohistochemical images of amyloid plaques in the hippocampus of 3×Tg-AD and WT mice are shown in Fig. 1A. As expected, the number and size of Aβ-immunopositive particles were markedly higher in the hippocampus of 3×Tg-AD mice (male or female) than in corresponding WT mice. Importantly, in the 3×Tg-AD mice, the number and size of Aβ-immunopositive particles in females were significantly higher than in males. Two-way ANOVA showed that gene mutation and sex difference had significant main effects and an interaction effect on amyloid plaque load in the hippocampus [gene mutation: $F(1, 36) = 7.154$, $P = 0.045$; sex difference: $F(1, 36) = 8.373$, $P = 0.041$; gene mutation × sex difference: $F(1, 36) = 6.541$, $P = 0.046$]. *Post hoc* Tukey's test (Fig. 1B) showed that the percentage area of Aβ in the 3×Tg-AD groups was significantly higher than in the WT groups ($P < 0.05$ for both). Further, in the 3×Tg-AD groups, the percentage area of Aβ in the females (7.6% ± 0.9%) was significantly greater ($P < 0.05$) than in the males (3.7% ± 0.8%).

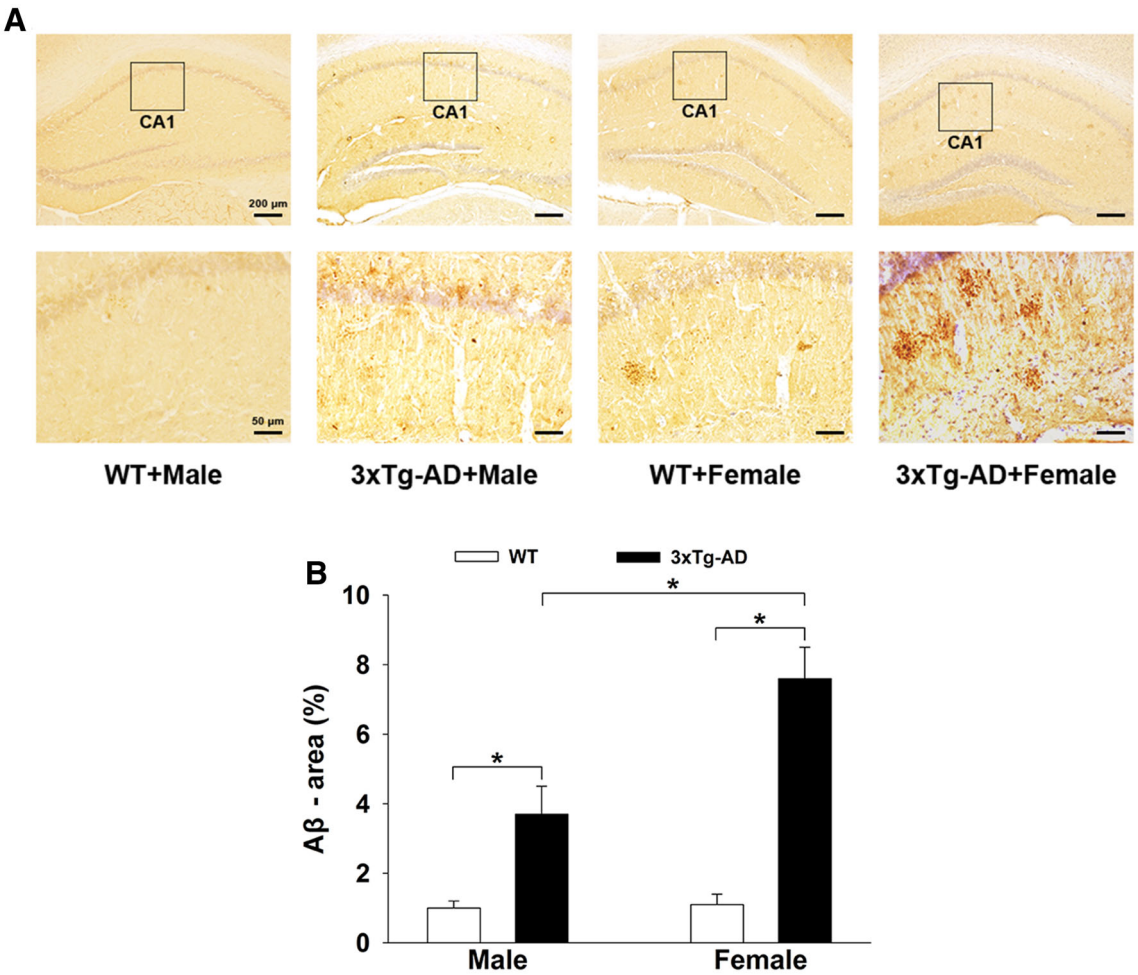

Fig. 1 Amyloid plaques in the hippocampus of 3×Tg-AD and WT mice. **A** Representative immunohistochemical images of amyloid plaques in both groups. **B** Histograms showing the percentage area of Aβ in the hippocampus was significantly higher in the 3×Tg-AD groups, especially in females (n = 6 mice/group; *$P < 0.05$).

Female 3×Tg-AD Mice Had More Neurofibrillary Tangles in the Hippocampus

The extent of neurofibrillary tangles is positively correlated with the severity of AD. It was evident that a high density of p-tau-positive staining and more p-tau-positive cells and dendrites occurred in the 3×Tg-AD groups, especially in females (Fig. 2A). Two-way ANOVA showed that gene mutation and sex difference had significant main effects and interaction effects on p-tau-positive cells in the hippocampus [gene mutation: $F(1, 36) = 8.342$, $P = 0.042$; sex difference: $F(1, 36) = 9.190$, $P = 0.034$; gene mutation × sex difference: $F(1, 36) = 9.217$, $P = 0.033$]. Tukey's *post hoc* test showed that the percentage of p-tau-positive cells in the hippocampus of 3×Tg-AD mice (male and female) was significantly higher than in WT mice ($P < 0.05$ for both; Fig. 2B). Moreover, the percentage of p-tau-positive cells in the 3×Tg-AD + Female group (95.3% ± 4.1%) was higher ($P < 0.05$) than that in the 3×Tg-AD + Male group (84.2% ± 3.2%). Similar results were found for the p-tau area measurements (Fig. 2C). Two-way ANOVA showed that gene mutation and sex difference had significant main effects and interaction effects on p-tau [gene mutation: $F(1, 36) = 7.988$, $P = 0.043$; sex difference: $F(1, 36) = 7.631$, $P = 0.044$; gene mutation × sex difference: $F(1, 36) = 9.004$, $P = 0.036$]. Tukey's *post hoc* test showed that the percentage area of p-tau in the hippocampus of 3×Tg-AD mice (male and female) was higher than in WT mice ($P < 0.05$ for both; Fig. 2C). Tukey's *post hoc* test showed a higher percentage area of p-tau in the hippocampus of 3×Tg-AD + Female mice (22.1% ± 2.1%, $P < 0.05$) than in the 3×Tg-AD + Male mice (16.3% ± 1.3%).

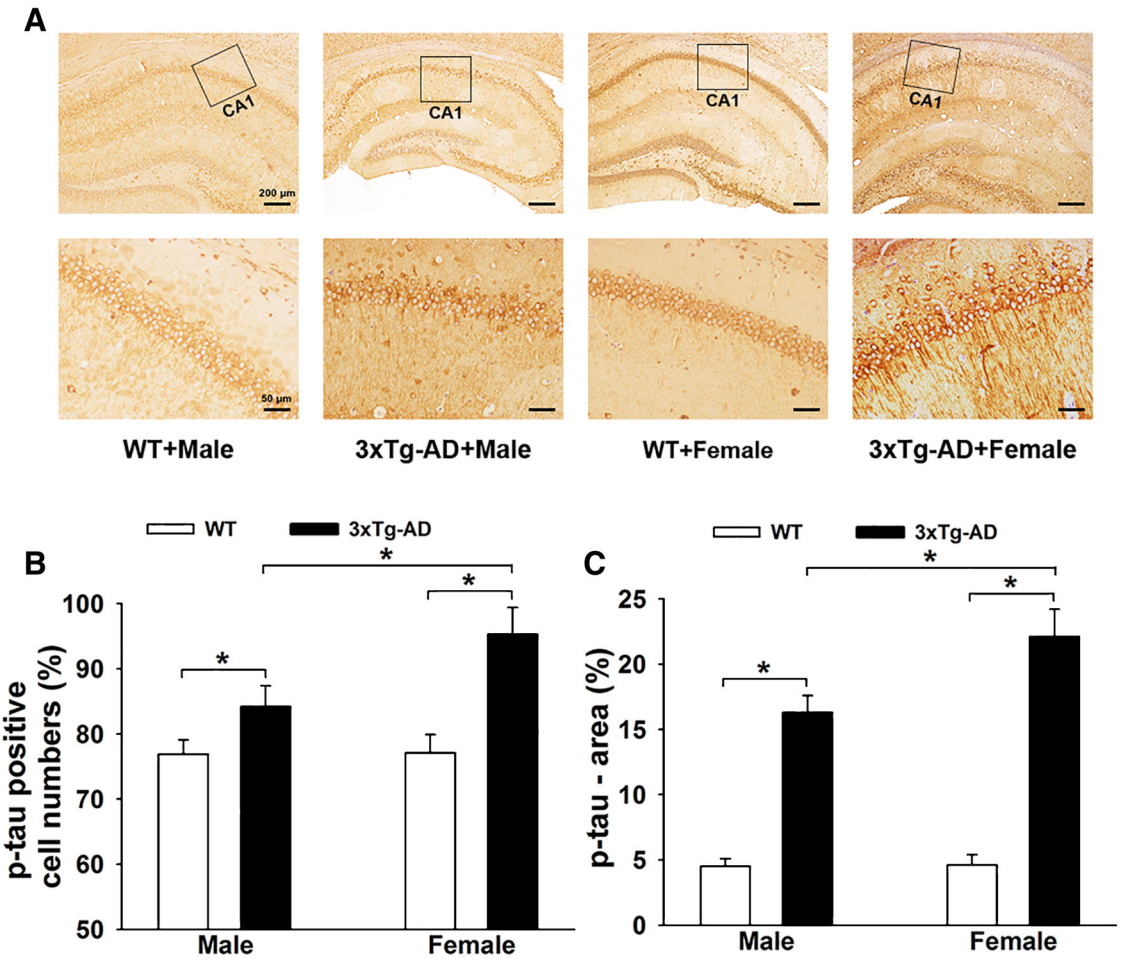

Fig. 2 Neurofibrillary tangles in the hippocampus of 3×Tg-AD and WT mice. **A** Representative immunohistochemical images of neurofibrillary tangles in both groups. **B** and **C** Histograms showing p-tau-positive cell numbers (**B**) and p-tau area (**C**), with significant increases in the 3×Tg-AD groups, especially in females (n = 6 mice/group; *$P < 0.05$).

Female 3×Tg-AD Mice Displayed Stronger Activation of Microglia and Astrocytes in the Hippocampus

Both Aβ and hyperphosphorylated tau protein can induce neuroinflammation. We found clear activation of microglia in the APP/PS1/tau mice, especially in females, with enhanced Iba-1 immunopositive optical density and increased area of Iba-1 (Fig. 3A). Two-way ANOVA showed that gene mutation and sex difference had significant main effects [gene mutation: $F(1, 36)$ = 10.02, P = 0.031; sex difference: F (1, 36) = 8.783, P = 0.037] and an interaction effect [gene mutation × sex difference: F (1, 36) = 9.452, P = 0.032] on the activation of microglia in the hippocampus. Tukey's *post hoc* test (Fig. 3B) showed that the percentage area of Iba-1 in the hippocampus of 3×Tg-AD mice (male and female) was higher than that in WT mice ($P < 0.05$ for both). Tukey's *post hoc* test indicated a higher ($P < 0.05$) percentage area of Iba-1 in the 3×Tg-AD + Female mice (14.9% ± 1.2%) than in 3×Tg-AD + Male mice (10.5% ± 1.0%). Similar to the microglial reaction, astrocytes were activated in the hippocampus of APP/PS1/tau mice (Fig. 4A). Two-way ANOVA showed that gene mutation and sex difference had significant main effects on the activation of astrocytes [gene mutation: $F(1, 36)$ = 8.53, P = 0.039; sex difference: $F(1, 36)$ = 9.05, P = 0.035; gene mutation × sex difference: $F(1, 36)$ = 8.772, P = 0.038]. Tukey's *post hoc* test (Fig. 4B) showed that the percentage area of GFAP in the hippocampus of 3×Tg-AD mice (male and female) was higher than in WT mice ($P < 0.05$ for both). Tukey's *post hoc* test showed a greater increment in GFAP area in the hippocampus of the APP/PS1/tau groups than the WT groups, higher ($P < 0.05$) in the 3×Tg-AD + Female group (22.6% ± 3.0%) than in the 3×Tg-AD + Male group (16.6% ± 1.8%).

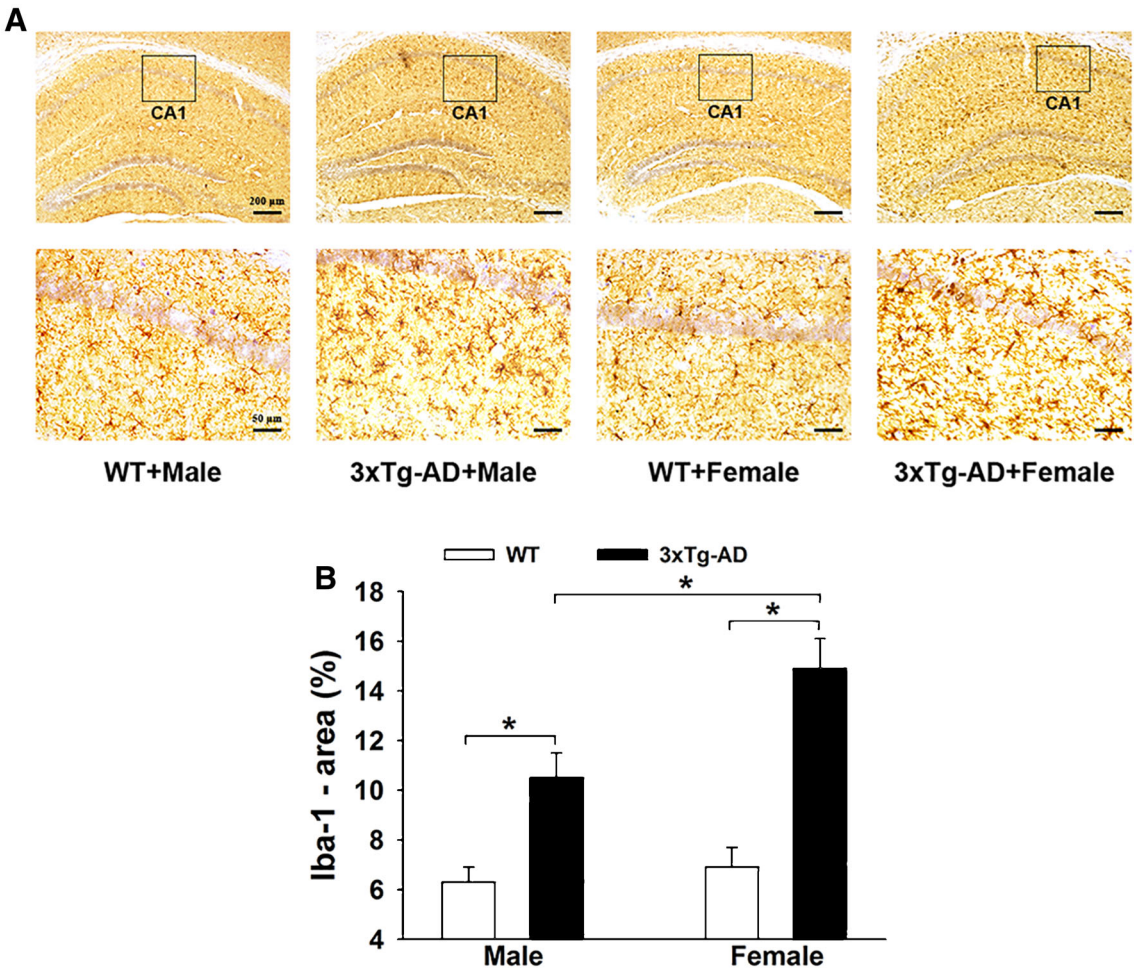

Fig. 3 Activation of microglia in the hippocampus of 3×Tg-AD and WT mice. **A** Representative immunohistochemical images of microglial activation in both groups. **B** Histograms showing the percentage areas of Iba-1 immunopositivity. Compared to the two WT groups, the percentage areas in both 3×Tg-AD groups were significantly higher. In the 3×Tg-AD groups, females showed greater microglial activation (n = 6/group; *$P < 0.05$).

Sex Differences in the PKA-CREB-MAPK signaling Pathway in the Hippocampus of 3×Tg-AD Mice

Considering that Aβ can affect hippocampal PKA-CREB-MAPK signaling, we further compared the sex differences in the PKA-CREB-MAPK signal molecules in the APP/PS1/tau mice. We found that the expression levels of p-PKA and p-CREB were markedly lower and p38-MAPK was higher in 3×Tg-AD mice (Fig. 5A–C). Two-way ANOVA indicated that gene mutation and sex difference had significant main effects and interaction effects on the levels of p-PKA and p-CREB [p-PKA: gene mutation, $F(1, 36) = 7.305$, $P = 0.045$; sex difference, $F(1, 36) = 8.397$, $P = 0.042$; gene mutation × sex difference, $F(1, 36) = 8.470$, $P = 0.041$; p-CREB: gene mutation, $F(1, 36) = 7.891$, $P = 0.043$; sex difference, $F(1, 36) = 9.056$, $P = 0.035$; gene mutation × sex difference, $F(1, 36) = 9.323$, $P = 0.032$]. Tukey's *Post hoc* tests showed that the levels of p-PKA (37.3% ± 5.3%) and p-CREB (29.7% ± 3.5%) in the 3×Tg-AD + Female group were lower than in the 3×Tg-AD + Male group (58.2% ± 4.9% and 48.7% ± 4.5%, $P < 0.05$; Fig. 5D, E). In contrast, p38-MAPK was clearly activated in the 3×Tg-AD mice (Fig. 5C). Two-way ANOVA showed that gene mutation and sex difference had significant main effects on the level of p-p38 [gene mutation: $F(1, 36) = 6.333$, $P = 0.047$; sex difference: $F(1, 36) = 8.436$, $P = 0.041$; gene mutation × sex difference: $F(1, 36) = 7.225$, $P = 0.045$]. With Tukey's *post hoc* test, the level of p-p38 in the 3×Tg-AD + Female mice (80.0% ± 3.3%) was higher than in the 3×Tg-AD + Male mice (71.2% ± 3.9%) ($P < 0.05$; Fig. 5F).

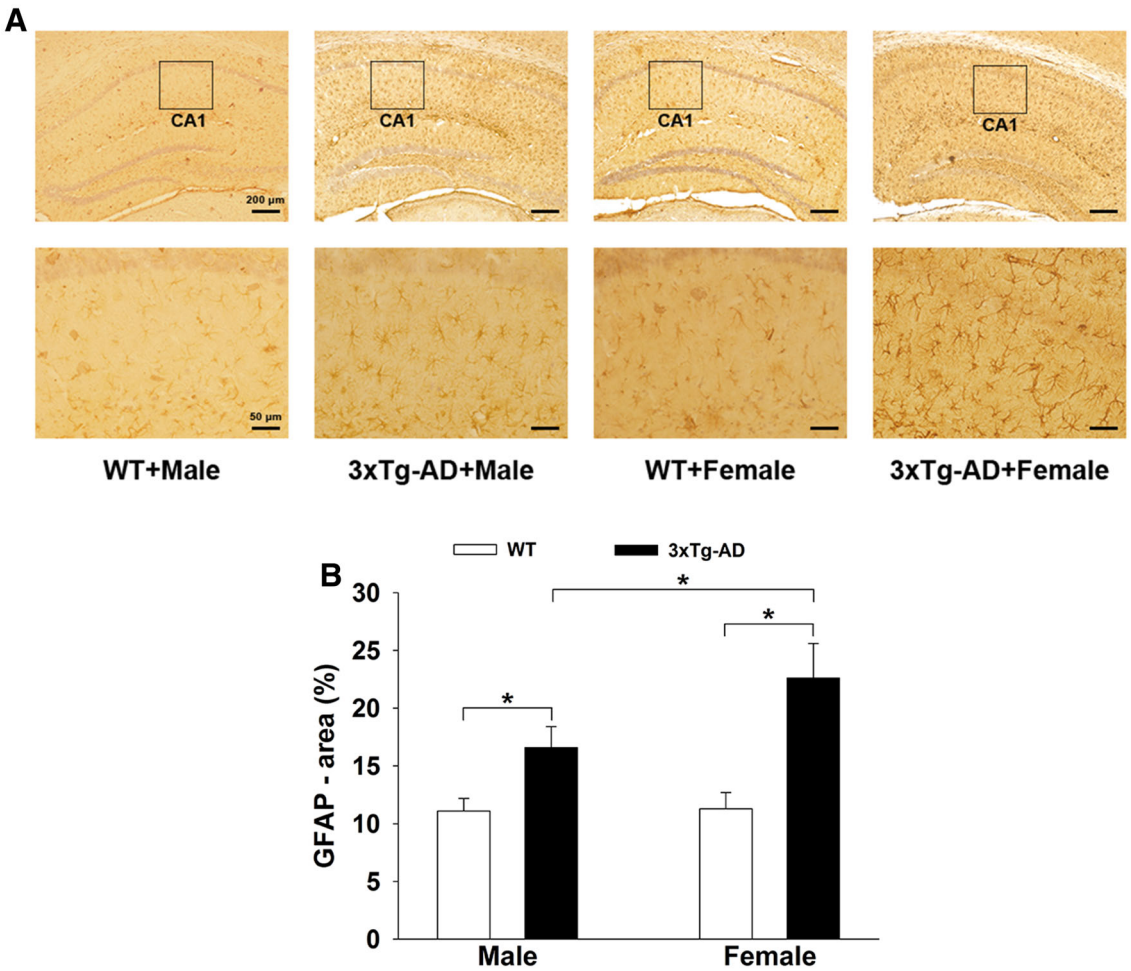

Fig. 4 Activation of astrocytes in the hippocampus of 3×Tg-AD and WT mice. **A** Representative immunohistochemical images of astrocytes in both groups. **B** Histograms showing the GFAP-immunopositive area in both groups. Similar to microglia, there was significant astrocyte activation in 3×Tg-AD males and females, especially in the latter (n = 6/group; *$P < 0.05$).

Female 3×Tg-AD Mice Exhibited Worse Cognitive Behaviors than Age- and Gene-Matched Male Mice in Morris Water Maze Tests

Based on the sex differences in the pathological features of 3×Tg-AD mice, we further found sex differences in cognitive function. The average escape latency in the hidden platform tests decreased with training [$F(4,148) = 84.150$; $P < 0.001$] (Fig. 6A). Two-way ANOVA showed that gene mutation and sex difference had significant effects on the average escape latency of all mice [gene mutation: $F(1, 37) = 17.797$, $P < 0.001$; sex difference: $F(1, 37) = 12.657$, $P = 0.001$; gene mutation × sex difference: $F(1, 37) = 5.823$, $P = 0.048$]. Tukey's *post hoc* test showed that the escape latency of female 3×Tg-AD mice (n = 10) was higher on training days 3 (50.60 ± 2.80 s, $P = 0.038$), 4 (41.10 ± 3.18 s, $P = 0.019$), and 5 (27.30 ± 3.53 s, $P = 0.021$) than of male 3×Tg-AD mice (40.95 ± 2.91 s on day 3, 32.15 ± 3.51 s on day 4, and 20.55 ± 3.53 s on day 5), indicating that the females had worse spatial learning than age-matched males. Representative swimming traces of mice in searching for the underwater platform on training day 4 are shown in Fig. 6C. In order to assess spatial memory, a probe trial was performed on day 6. Two-way ANOVA showed that gene and sex had significant effects on the swimming time in the target quadrant [gene mutation: $F(1, 36) = 21.695$, $P < 0.001$; sex difference: $F(1, 36) = 14.067$, $P = 0.001$; gene mutation × sex difference: $F(1, 36) = 4.322$, $P = 0.045$] (Fig. 6B). Tukey's *post hoc* test showed that the target quadrant swimming time in female 3×Tg-AD mice (12.46% ± 3.75%, $P = 0.001$, n = 10) was significantly lower than in male 3×Tg-AD mice (35.06% ± 3.54%, n = 10), indicating that the females had worse spatial memory than age-matched males.

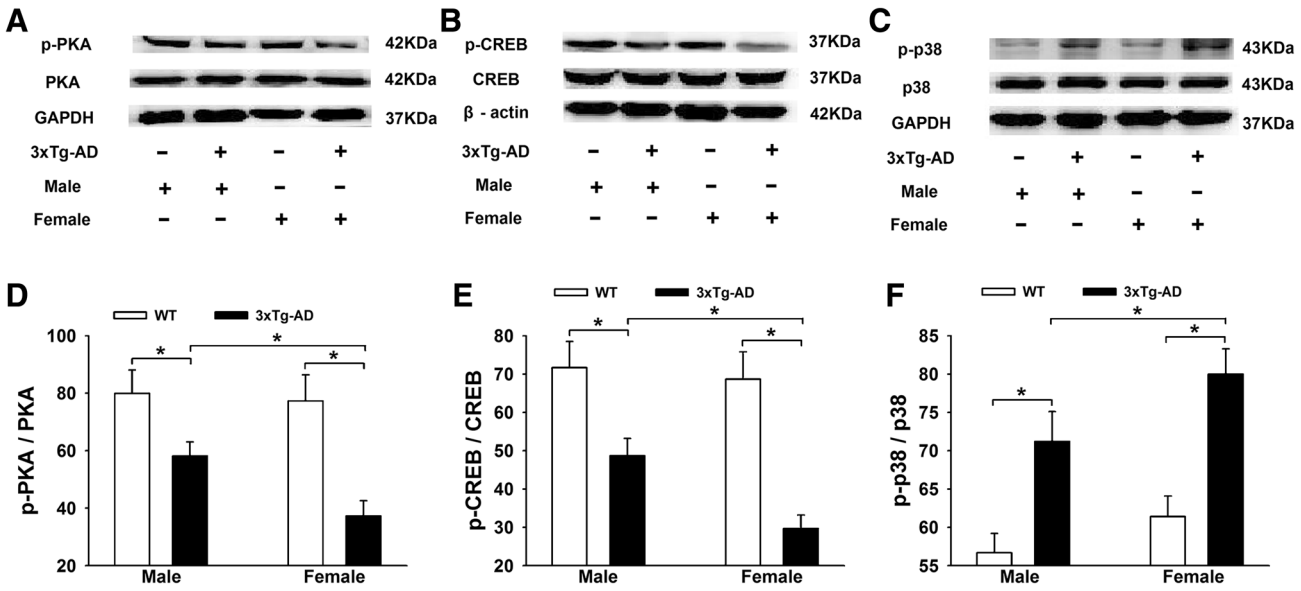

Fig. 5 Sex differences in the hippocampal PKA-CREB-MAPK signal molecules in 3×Tg-AD and WT mice. **A–C** Representative Western blots showing the expression levels of p-PKA (**A**), p-CREB (**B**), and p-p38 (**C**). **D** and **E** Histograms showing the statistical analysis of p-PKA and p-CREB, with a significant decrease in the percentages of p-PKA/PKA and p-CREB/CREB in the 3×Tg-AD groups, especially in females. **F** Histograms showing statistical analysis of the p-p38 level, with a significant increase in the percentages of p-p38/p38 in the 3×Tg-AD groups, especially in females (n = 6/group; $^*P < 0.05$).

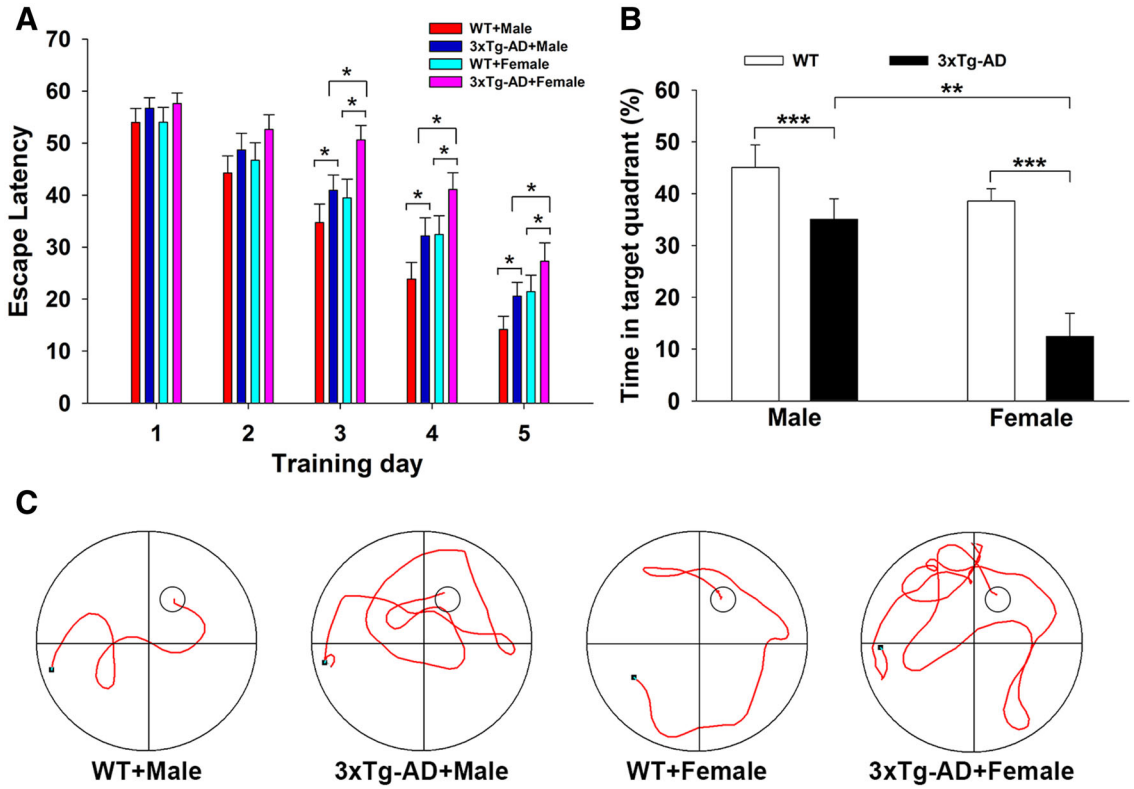

Fig. 6 Female 3×Tg-AD mice exhibited worse cognitive behaviors than age- and gene-matched males in Morris water maze tests. **A** Plots showing the average escape latencies during 5 continuous days of acquisition trials ($^*P < 0.05$). **B** Histograms showing the percentage of time spent in the target quadrant in probe trials ($^{**}P < 0.01$, $^{***}P < 0.001$). **C** Representative swimming tracks on training day 4 in hidden platform tests (large circles, water maze pool; small circles, platform; black dots, starting points; n = 10/group).

Discussion

APP/PS1/tau 3×Tg-AD mice exhibit amyloid plaques and neurofibrillary tangles at 12–15 months [14] and these pathological changes match the profiles of AD patients [15]. The APP/PS1/tau 3×Tg-AD mice may be superior to the APP/PS1 dual transgenic mice, because the latter are relatively deficient in the pathology of hyperphosphorylated tau protein, an important characteristic correlated with the severity of dementia in AD. To systematically investigate the pathological characteristics, including neurofibrillary tangles, we used 12-month-old APP/PS1/tau 3×Tg-AD mice as the animal model.

Sex differences in the prevalence, risk, and severity of AD have been demonstrated in numerous clinical and epidemiological studies. Animal research with mouse models of AD also supports the greater susceptibility to AD in females. For example, it has recently been reported that female APP/PS1 AD mice have more severe cognitive impairments than males [16]; females have a higher Aβ burden as well as greater neuronal and synaptic degeneration than males; and the levels of pro-inflammatory cytokines such as IL-1β and TNF-α in the brain of female APP/PS1 mice are all higher than those in males [17]. Consistent with these results, our findings revealed that female APP/PS1/tau 3×Tg-AD mice not only carried a more dramatic amyloid plaque load, more marked neurofibrillary tangle aggregation, and stronger neuroinflammation in the hippocampus, but also worse cognitive behaviors in the MWM test than age- and gene-matched males. Therefore, the full sex differences in AD pathophysiology, including tau protein, are well displayed in 12-month-old APP/PS1/tau 3×Tg-AD mice. The more serious pathology in the female 3×Tg-AD mice could explain why the cognitive behaviors of 3×Tg-AD mice are worse in females than in males [18].

All of the AD biomarkers, including Aβ plaques, phosphorylated tau, and neuroinflammation in the brain, are closely associated with the down-regulation of PKA-CREB and up-regulation of the p38-MAPK signaling pathway [19]. It is known that PKA physiologically activated by cAMP enters the nucleus and thereby activates the CREB transcription factor (P-CREB) [20]. The PKA-CREB pathway is vital for synaptic plasticity and memory formation [21–24], and is crucial for the maintenance of long-term potentiation [25, 26]. So, the downregulation of cAMP-PKA-CREB activity is closely associated with impairments in cognition and memory [21, 27–29]. This finding is consistent with reports showing decreased PKA and CREB activity in the AD brain [30–32]. In fact, Aβ toxicity in AD has been attributed to impairment of the PKA/CREB pathway [33] by decreasing p-PKA and p-CREB in hippocampal neurons [34] and inhibiting CREB-regulated transcription coactivator 1 (CRTC1) [35]. In addition, it has been reported that $A\beta_{1-40}$ treatment induces time-dependent activation of p38-MAPK in hCMEC/D3 cells [36]. The P38-MAPK pathway mainly participates in tau phosphorylation [37] and neuroinflammatory responses such as IL-6 secretion [38], which in turn aggravates Aβ pathology. So, the activation of p38-MAPK in neuronal cells is closely associated with the tau hyperphosphorylation, neuronal inflammation, and memory loss in AD [39–41]. In the present study, we found that the expression levels of p-PKA and p-CREB in the hippocampus were lower, while p-p38-MAPK was higher in 3×Tg-AD mice, especially in females, and this probably accounts for the more serious cerebral pathology and behavioral impairments in female 3×Tg-AD mice.

An important primary mechanism involved in the more serious pathological damage and behavioral deficits in females could be the decline of estrogen in the AD mice. It is well known that estrogen and its receptors play multiple key neuroprotective roles in preventing a variety of neurodegenerative disorders, including AD. For example, estrogen protects against the toxicity of Aβ by promoting the non-amyloidogenic metabolism of APP [42, 43]; promotes the health of cholinergic neurons by increasing cholinergic activity [44, 45]; has antioxidant [46] and anti-inflammatory properties [47]; significantly increases axonal outgrowth and dendritic spines in cultured mouse hippocampal neurons [48, 49]; significantly increases the amplitude of long-term potentiation in hippocampal slices [50]; and increases neurogenesis in various brain regions such as the hippocampus. We noted that 12-month-old female mice have reached reproductive senescence and the estrogen level has significantly decreased [18]. Therefore, the neuroprotective effects of estrogen on the 12-month-old female mice in the present study were sharply reduced, exposing them to a variety of insults such as the neurotoxic Aβ and p-tau. This probably forms the basis of the more serious AD pathology in females. Therefore, maintaining estrogen synthesis might be critically important for reducing the risk of AD in females. In fact, estrogen replacement therapy (ERT) has been assessed. Most recently, Christensen *et al*. [51] reported that 17β-estradiol (E2) treatment for four months in 7–9 month-old female 3×Tg-AD mice significantly decreases the Aβ load in the hippocampus and improves cognitive performance in the Y maze. Continuation of ERT appears to be effective in protecting cognition in women with a heightened risk for AD when initiated close to the onset of menopause [52]. We are currently performing an ERT experiment with E2 in bilaterally ovariectomized 3×Tg-AD female mice, and have found that ERT decreases the escape latency and increases

the target zone swimming time in the MWM test, suggesting that ERT improves spatial learning and memory in female AD mice (data not shown). Other phenotypes such as Aβ pathology and neuroinflammation are being investigated. The neuroprotection by estrogen is mediated partly through activation of the PKA-CREB and inhibition of the p38-MAPK signaling pathways [53–55]. These results are consistent with and support our findings that the levels of p-PKA and p-CREB were significantly lower, while p38-MAPK was significantly activated in 12-month-old female 3×Tg-AD mice.

In summary, we systematically investigated sex differences in the neuropathology and cognitive function in 12-month-old 3×Tg-AD mice. Compared to males, the females exhibited more prominent pathological characteristics including not only extracellular Aβ plaques but also intracellular neurofibrillary tangles and neuroinflammation in the hippocampus, as well as worse behavior in the MWM test. A PKA-CREB-MAPK signaling disorder induced by estrogen deficiency in the 12-month-old female 3×Tg-AD mice might be involved in the more serious pathological damage and worse cognitive deficits in the female AD mice. Therefore, we suggest that sex differences should be taken into account when examining the pathological characteristics of AD and related target molecules. Furthermore, estrogen supplementation or PKA-CREB-MAPK signal stabilization could be beneficial in relieving the pathological damage and behavioral deficits of AD in reproductively senescent females.

Acknowledgements We gratefully acknowledge the participants for their generous dedication to the experiment. This work was partially funded by "Sanjin Scholars" of Shanxi Province and the National Natural Science Foundation of China (31471080, 31600865, and 31700918). It was sponsored by the Fund for Shanxi Key Subjects Construction, Shanxi "1331 Project" Key Subjects Construction, and Key Laboratory of Cellular Physiology (Shanxi Medical University) in Shanxi Province.

Compliance with Ethical Standards

Conflict of interest All authors claim that there is no conflict of interest.

References

1. Grimm MO, Mett J, Grimm HS, Hartmann T. APP function and lipids: a bidirectional link. Front Mol Neurosci 2017, 10: 63.
2. Kim NY, Cho MH, Won SH, Kang HJ, Yoon SY, Kim DH. Sorting nexin-4 regulates beta-amyloid production by modulating beta-site-activating cleavage enzyme-1. Alzheimers Res Ther 2017, 9: 4.
3. Chen YC. Impact of a discordant helix on beta-amyloid structure, aggregation ability and toxicity. Eur Biophys J 2017, 46: 681–687.
4. Collin L, Bohrmann B, Gopfert U, Oroszlan-Szovik K, Ozmen L, Gruninger F. Neuronal uptake of tau/pS422 antibody and reduced progression of tau pathology in a mouse model of Alzheimer's disease. Brain 2014, 137: 2834–2846.
5. Wilcock GK, Esiri MM. Plaques, tangles and dementia. A quantitative study. J Neurol Sci 1982, 56: 343–356.
6. Leyns CEG, Holtzman DM. Glial contributions to neurodegeneration in tauopathies. Mol Neurodegener 2017, 12: 50.
7. Dye RV, Miller KJ, Singer EJ, Levine AJ. Hormone replacement therapy and risk for neurodegenerative diseases. Int J Alzheimers Dis 2012, 2012: 258454.
8. Phung TK, Waltoft BL, Laursen TM, Settnes A, Kessing LV, Mortensen PB, *et al.* Hysterectomy, oophorectomy and risk of dementia: a nationwide historical cohort study. Dement Geriatr Cogn Disord 2010, 30: 43–50.
9. Koran MEI, Wagener M, Hohman TJ, Alzheimer's Neuroimaging I. Sex differences in the association between AD biomarkers and cognitive decline. Brain Imaging Behav 2017, 11: 205–213.
10. Koppel J, Acker C, Davies P, Lopez OL, Jimenez H, Azose M, *et al.* Psychotic Alzheimer's disease is associated with gender-specific tau phosphorylation abnormalities. Neurobiol Aging 2014, 35: 2021–2028.
11. Carroll JC, Rosario ER, Kreimer S, Villamagna A, Gentzschein E, Stanczyk FZ, *et al.* Sex differences in beta-amyloid accumulation in 3xTg-AD mice: role of neonatal sex steroid hormone exposure. Brain Res 2010, 1366: 233–245.
12. Hirata-Fukae C, Li HF, Hoe HS, Gray AJ, Minami SS, Hamada K, *et al.* Females exhibit more extensive amyloid, but not tau, pathology in an Alzheimer transgenic model. Brain Res 2008, 1216: 92–103.
13. Chen YJ, Liu YL, Zhong Q, Yu YF, Su HL, Toque HA, *et al.* Tetrahydropalmatine protects against methamphetamine-induced spatial learning and memory impairment in mice. Neurosci Bull 2012, 28: 222–232.
14. Yang SH, Kim J, Lee MJ, Kim Y. Abnormalities of plasma cytokines and spleen in senile APP/PS1/Tau transgenic mouse model. Sci Rep 2015, 5: 15703.
15. Bertoni-Freddari C, Sensi SL, Giorgetti B, Balietti M, Di Stefano G, Canzoniero LM, *et al.* Decreased presence of perforated synapses in a triple-transgenic mouse model of Alzheimer's disease. Rejuvenation Res 2008, 11: 309–313.
16. Laws KR, Irvine K, Gale TM. Sex differences in cognitive impairment in Alzheimer's disease. World J Psychiatry 2016, 6: 54–65.
17. Jiao SS, Bu XL, Liu YH, Zhu C, Wang QH, Shen LL, *et al.* Sex dimorphism profile of Alzheimer's disease-type pathologies in an APP/PS1 mouse model. Neurotox Res 2016, 29: 256–266.
18. Clinton LK, Billings LM, Green KN, Caccamo A, Ngo J, Oddo S, *et al.* Age-dependent sexual dimorphism in cognition and stress response in the 3xTg-AD mice. Neurobiol Dis 2007, 28: 76–82.
19. Han WN, Holscher C, Yuan L, Yang W, Wang XH, Wu MN, *et al.* Liraglutide protects against amyloid-beta protein-induced impairment of spatial learning and memory in rats. Neurobiol Aging 2013, 34: 576–588.
20. Li B, He X, Sun Y, Li B. Developmental exposure to paraquat and maneb can impair cognition, learning and memory in Sprague-Dawley rats. Mol Biosyst 2016, 12: 3088–3097.
21. Yamamoto-Sasaki M, Ozawa H, Saito T, Rosler M, Riederer P. Impaired phosphorylation of cyclic AMP response element binding protein in the hippocampus of dementia of the Alzheimer type. Brain Res 1999, 824: 300–303.
22. Tully T, Bourtchouladze R, Scott R, Tallman J. Targeting the CREB pathway for memory enhancers. Nat Rev Drug Discov 2003, 2: 267–277.

23. Josselyn SA, Nguyen PV. CREB, synapses and memory disorders: past progress and future challenges. Curr Drug Targets CNS Neurol Disord 2005, 4: 481–497.
24. Chen Y, Huang X, Zhang YW, Rockenstein E, Bu G, Golde TE, *et al.* Alzheimer's beta-secretase (BACE1) regulates the cAMP/PKA/CREB pathway independently of beta-amyloid. J Neurosci 2012, 32: 11390–11395.
25. Ran I, Laplante I, Lacaille JC. CREB-dependent transcriptional control and quantal changes in persistent long-term potentiation in hippocampal interneurons. J Neurosci 2012, 32: 6335–6350.
26. Yin JC, Tully T. CREB and the formation of long-term memory. Curr Opin Neurobiol 1996, 6: 264–268.
27. Gong B, Vitolo OV, Trinchese F, Liu S, Shelanski M, Arancio O. Persistent improvement in synaptic and cognitive functions in an Alzheimer mouse model after rolipram treatment. J Clin Invest 2004, 114: 1624–1634.
28. Puzzo D, Vitolo O, Trinchese F, Jacob JP, Palmeri A, Arancio O. Amyloid-beta peptide inhibits activation of the nitric oxide/cGMP/cAMP-responsive element-binding protein pathway during hippocampal synaptic plasticity. J Neurosci 2005, 25: 6887–6897.
29. Matsuzaki K, Yamakuni T, Hashimoto M, Haque AM, Shido O, Mimaki Y, *et al.* Nobiletin restoring beta-amyloid-impaired CREB phosphorylation rescues memory deterioration in Alzheimer's disease model rats. Neurosci Lett 2006, 400: 230–234.
30. Kim SH, Nairn AC, Cairns N, Lubec G. Decreased levels of ARPP-19 and PKA in brains of Down syndrome and Alzheimer's disease. J Neural Transm Suppl 2001: 263–272.
31. Sanchez-Mut JV, Aso E, Heyn H, Matsuda T, Bock C, Ferrer I, *et al.* Promoter hypermethylation of the phosphatase DUSP22 mediates PKA-dependent TAU phosphorylation and CREB activation in Alzheimer's disease. Hippocampus 2014, 24: 363–368.
32. Saura CA, Valero J. The role of CREB signaling in Alzheimer's disease and other cognitive disorders. Rev Neurosci 2011, 22: 153–169.
33. Tong L, Thornton PL, Balazs R, Cotman CW. Beta-amyloid-(1-42) impairs activity-dependent cAMP-response element-binding protein signaling in neurons at concentrations in which cell survival Is not compromised. J Biol Chem 2001, 276: 17301–17306.
34. Vitolo OV, Sant'Angelo A, Costanzo V, Battaglia F, Arancio O, Shelanski M. Amyloid beta-peptide inhibition of the PKA/CREB pathway and long-term potentiation: reversibility by drugs that enhance cAMP signaling. Proc Natl Acad Sci U S A 2002, 99: 13217–13221.
35. Espana J, Valero J, Minano-Molina AJ, Masgrau R, Martin E, Guardia-Laguarta C, *et al.* beta-Amyloid disrupts activity-dependent gene transcription required for memory through the CREB coactivator CRTC1. J Neurosci 2010, 30: 9402–9410.
36. Tai LM, Holloway KA, Male DK, Loughlin AJ, Romero IA. Amyloid-beta-induced occludin down-regulation and increased permeability in human brain endothelial cells is mediated by MAPK activation. J Cell Mol Med 2010, 14: 1101–1112.
37. Kuo YC, Tsao CW. Neuroprotection against apoptosis of SK-N-MC cells using RMP-7- and lactoferrin-grafted liposomes carrying quercetin. Int J Nanomedicine 2017, 12: 2857–2869.
38. Wan Z, Mah D, Simtchouk S, Klegeris A, Little JP. Globular adiponectin induces a pro-inflammatory response in human astrocytic cells. Biochem Biophys Res Commun 2014, 446: 37–42.
39. Ghasemi R, Zarifkar A, Rastegar K, maghsoudi N, Moosavi M. Insulin protects against Abeta-induced spatial memory impairment, hippocampal apoptosis and MAPKs signaling disruption. Neuropharmacology 2014, 85: 113–120.
40. Ghasemi R, Zarifkar A, Rastegar K, Maghsoudi N, Moosavi M. Repeated intra-hippocampal injection of beta-amyloid 25-35 induces a reproducible impairment of learning and memory: considering caspase-3 and MAPKs activity. Eur J Pharmacol 2014, 726: 33–40.
41. Yao Y, Huang JZ, Chen L, Chen Y, Li X. In vivo and in vitro studies on the roles of p38 mitogen-activated protein kinase and NADPH-cytochrome P450 reductase in Alzheimer's disease. Exp Ther Med 2017, 14: 4755–4760.
42. Schupf N, Lee JH, Pang D, Zigman WB, Tycko B, Krinsky-McHale S, *et al.* Epidemiology of estrogen and dementia in women with Down syndrome. Free Radic Biol Med 2018, 114: 62–68.
43. Goodman Y, Bruce AJ, Cheng B, Mattson MP. Estrogens attenuate and corticosterone exacerbates excitotoxicity, oxidative injury, and amyloid beta-peptide toxicity in hippocampal neurons. J Neurochem 1996, 66: 1836–1844.
44. Luine VN. Estradiol increases choline acetyltransferase activity in specific basal forebrain nuclei and projection areas of female rats. Exp Neurol 1985, 89: 484–490.
45. Lambert JC, Harris JM, Mann D, Lemmon H, Coates J, Cumming A, *et al.* Are the estrogen receptors involved in Alzheimer's disease? Neurosci Lett 2001, 306: 193–197.
46. Behl C, Widmann M, Trapp T, Holsboer F. 17-beta estradiol protects neurons from oxidative stress-induced cell death in vitro. Biochem Biophys Res Commun 1995, 216: 473–482.
47. Bruce-Keller AJ, Keeling JL, Keller JN, Huang FF, Camondola S, Mattson MP. Antiinflammatory effects of estrogen on microglial activation. Endocrinology 2000, 141: 3646–3656.
48. Fester L, Prange-Kiel J, Jarry H, Rune GM. Estrogen synthesis in the hippocampus. Cell Tissue Res 2011, 345: 285–294.
49. Mukai H, Kimoto T, Hojo Y, Kawato S, Murakami G, Higo S, *et al.* Modulation of synaptic plasticity by brain estrogen in the hippocampus. Biochim Biophys Acta 2010, 1800: 1030–1044.
50. Grassi S, Tozzi A, Costa C, Tantucci M, Colcelli E, Scarduzio M, *et al.* Neural 17beta-estradiol facilitates long-term potentiation in the hippocampal CA1 region. Neuroscience 2011, 192: 67–73.
51. Christensen A, Pike CJ. Age-dependent regulation of obesity and Alzheimer-related outcomes by hormone therapy in female 3xTg-AD mice. PLoS One 2017, 12: e0178490.
52. Wroolie TE, Kenna HA, Williams KE, Rasgon NL. Cognitive effects of hormone therapy continuation or discontinuation in a sample of women at risk for Alzheimer disease. Am J Geriatr Psychiatry 2015, 23: 1117–1126.
53. Lan YL, Zhao J, Li S. Update on the neuroprotective effect of estrogen receptor alpha against Alzheimer's disease. J Alzheimers Dis 2015, 43: 1137–1148.
54. Pratap UP, Patil A, Sharma HR, Hima L, Chockalingam R, Hariharan MM, *et al.* Estrogen-induced neuroprotective and anti-inflammatory effects are dependent on the brain areas of middle-aged female rats. Brain Res Bull 2016, 124: 238–253.
55. Huff MO, Todd SL, Smith AL, Elpers JT, Smith AP, Murphy RD, *et al.* Arsenite and Cadmium activate MAPK/ERK via membrane estrogen receptors and G-protein coupled estrogen receptor signaling in human lung adenocarcinoma cells. Toxicol Sci 2016, 152: 62–71.